Hindawi
Advances in Civil Engineering
Volume 2019, Article ID 2424518, 14 pages
https://doi.org/10.1155/2019/2424518

Research Article

Experimental Study on Flexural Behavior of Prestressed Concrete Beams Reinforced by CFRP under Chloride Environment

Yunyan Liu and Yingfang Fan

College of Transportation Engineering, Dalian Maritime University, Dalian 116026, China

Correspondence should be addressed to Yingfang Fan; fanyf72@aliyun.com

Received 5 May 2019; Revised 15 July 2019; Accepted 24 July 2019; Published 29 August 2019

Guest Editor: Charis Apostolopoulos

In order to study the effects of initial damages, CFRP reinforcement, and chloride corrosion on the flexural behavior of prestressed concrete beams, ten prestressed concrete beams were designed and manufactured, which were preloaded with 0%, 40%, and 60% of the ultimate load to crack. Then, part of the beams were reinforced by CFRP and immersed in chloride condition for 120 days. After that, the four-point bending tests were performed. Then, the sectional strain, deformation, flexural stiffness, flexural capacity, ductility, and the cracking characteristics were researched. The test results demonstrate that the sectional strain of PC beams still follows the plane cross section assumption after a pure bending deformation considering of the initial cracks, chloride corrosion, and CFRP reinforcement. The initial damage accelerates the chloride corrosion, resulting in the loss of initial stiffness, ductility, and cracking load, and the reduction in flexural capacity is less than 10%, and the failure modes of these beams are prone to change from concrete crushing to shear failure. In the cracking stage, the reinforcement of CFRP inhibits the bending deformation, leading to the reduction in stiffness degradation rates and the increase of cracking load, and the ultimate load increases by 12.8%~18.7%. The reinforcement of CFRP constrains the development of cracks, increases the cracks numbers by 50%~130%, decreases the cracking rates of beam bottoms by 52.5%, and reduces the average crack widths by 65.8% at 195 kN. It can be seen that the reinforcing effect of CFRP is more significant compared with the weakening effect of short-term chloride corrosion and initial damage on the flexural behavior.

1. Introduction

Prestressed concrete structure has been widely promoted because of its high strength, excellent performance, and structure diversification. Also, these structures are more prone to be affected by the environment due to its composition and mechanical characteristics, such as high temperature, freezing, acid rain, and deicing salt corrosion. Chloride corrosion is the major influencing factor. Nowadays, the durability problems of these structures occur frequently, which needs to be replaced, repaired, and strengthened. The Sorell Causeway Bridge [1] in Australia was demolished, and the "S.Stefano" viaduct [2] in Italy collapsed suddenly, following the corrosion of prestressing tendons in the beams, due to the long-term exposure to an aggressive marine environment. Prestressing steel subjected to high permanent stress has generally poor resistance to corrosion [3] compared to the ordinary steel bar. The loss of cross area and mechanical behavior of steel strands and the degradation of bond behavior between concrete and steel strands [4–6] will have a significant influence on the safety of prestressed concrete structures. Li and Yuan [7] believed that the effect of slight corrosion rates (less than 2.87%) is not significant to the flexural capacity, but will lead to the remarkable degradation of ultimate deflection for the beams with wire rupture failure. The tests of Rinaldi et al. [8] and Zhang et al. [9] show that the ultimate capacity of PC beams decreases with the increase of corrosion degree and turns the failure mode from ductile to brittle. An analysis model is proposed by Wang et al. [5] to predict the failure and flexural strength of PC beams under chloride corrosion condition. A numerical model is proposed by Coronelli to simulate the

effects of wire breaking in PC beams suffering from corrosion condition. Also, the local fracture of corroded steel strand in different locations in PC beam is simulated by Yang et al. [10] through a rapid corrosion test, and the test results show that the closer the corrosion fracture location is to the midspan, the more obvious the reduction in flexural stiffness and capacity is.

In practical engineering, the bridge is not only affected by the environment but also by fatigue loads. Some factors like low design standards overloaded for a long time or the vehicles' impact may lead to the damage on concrete bridges. The steels in the cracking area are always in a high stress state, even if the beam was unloaded completely, and there will be the residual cracks and deflection. The tests of Vicente et al. [11] and Recupero and Spinella [12] indicate that cracking and internal damage caused by cyclic loading will affect the bond behavior between steel strand and concrete, reduce the stiffness and natural frequency, and increase the vertical deflection and crack widths. The tests of Dasar et al. [13] show that the bending cracks of reinforced concrete beams exposed to the marine environment for a long time accelerate the corrosion rate of the steel, reduce the effective prestress and flexural capacity, and lead to the earlier failure.

Carbon fiber composite (CFRP) has the advantages of lightweight, high strength, corrosion resistance, and fatigue resistance. Therefore, CFRP is widely used to strength and repair damaged bridges, while greatly reducing installation time and cost [14]. At present, the reinforcement of corroded prestressed concrete structures by CFRP has attracted much attention. Adham and Khaled [15] hold that the flexural capacity of corroded prestressed concrete beams can be restored after CFRP repaired, but the reduction in ductility is irreversible. Shaw and Andrawes [16] repaired a corroded PC beam by mortar, GFRP, and CFRP, the results show that the mortar repair is alone insufficient in regaining the concrete initial strength and stiffness, and CFRP laminates are superior to GFRP laminates in regaining the stiffness and flexural capacity. The reinforcement of CFRP to prestressed concrete beams with damages has also been concerned by many scholars [17–20]. It is thought that the bearing capacity and stiffness of beams with damages due to overload and vehicle impact can be effectively restored after the CFRP reinforcement. At present, there are few research studies on the CFRP reinforcement of prestressed concrete beams with bending cracks and exposed to chloride environments, and such damage condition is more close to the actual project and more worthy to be studied.

The four-point bending tests were applied on all test beams. And the effects of CFRP reinforcement, initial bending cracks, and chloride corrosion on the distribution of cross-sectional strain, structural deformation, flexural stiffness, flexural capacity, crack propagation, and failure modes were researched.

2. Experimental Programs

2.1. Concrete Specimens. Ten pretensioned prestressed concrete beams were designed and manufactured. Commercial concrete was adopted, and the concrete strength grade was C40. All beams have the same dimension of $150 \times 250 \times 2200$ mm. The beams were reinforced by four 14 mm deformed bars at top and bottom and seven 6 mm stirrups with 100 mm at beam end. The beams were pretensioned with two 12.7 mm strands, and the initial prestress of the strand is 558 MPa, which is about 0.3 times of the yield strength. The details are shown in Figure 1.

The average yield strength of the prestressed strand, the deformed bars, and the 6 mm plain bars was 1860 MPa, 335 MPa, and 235 MPa, respectively, and the elastic modulus was 195 GPa, 200 GPa, and 210 GPa, respectively. The average compressive strength of 28-day concrete for all the beams was 49.4 MPa.

2.2. Test Condition. In order to simulate the influence of initial cracks, CFRP reinforcement, and chloride corrosion on the flexural behavior of PC beams, ten beams were applied different loading conditions, respectively. The test conditions of all beams are listed in Table 1.

In order to simulate the influence of initial damage on the durability of PC beams, six beams were preloaded to crack with 40% and 60% of the ultimate load. The distributions and parameters of initial cracks are shown in Figure 2 and Table 2.

Then, the beams were reinforced by CFRP, and U-shaped hoops were set at both ends, such as beam C0-1, C40-1, C60-1, C0-2, C40-2, and C60-2. The reinforcing scheme of CFRP is shown in Figure 3, and the mechanical properties of CFRP are shown in Table 3.

After preloading and CFRP reinforcement, the beams were immersed in a deicing salt solution for 120 days. The components of the solution are $CaCl_2$ and $MgCl_2$, and the concentration is 5%. It can be seen in Figure 4.

2.3. Loading Process. The actions of multifactor, such as initial damage, CFRP reinforcement, and chloride corrosion, change the bond performance between steel bars and concrete and affect the propagation of bending cracks. The design codes are very difficult to predict the flexural behavior and crack widths of these PC beams. The four-point bending tests were employed to study the effects of multifactor on the flexural behavior in the current study. Each beam was simply supported and had a pure bending span of 600 mm and two shear spans of 600 mm. Figure 5 shows the details of loading setup.

The loading process was divided into two stages. The first stage was controlled by load until reaching 85% of the ultimate load of the control beam. The load was applied step by step at a rate of 5 kN per step until crack load, then the rate was 10 kN per step. The second stage was controlled by deflection, and the loading increment was 0.6 mm per step. The loading test was stopped when the carrying capacity dropped to 75% of the ultimate load.

The vertical deflections at the midspan were measured by a displacement sensor. Electrical resistance strain gauges were pasted on the midspan section to measure concrete strains. Arrangement of the gauges is shown in Figure 5. One

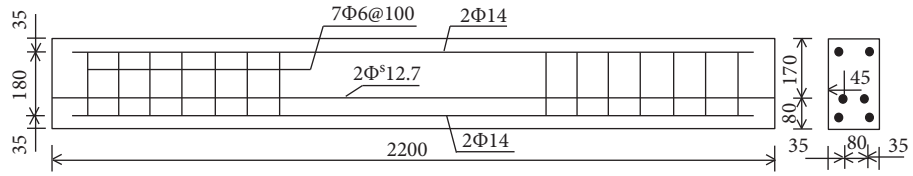

Figure 1: Beam details (unit: mm).

Table 1: Test conditions.

Beam	Preloading (kN)	Reinforcement	Environment condition
A1	0	—	—
C0-3	0		
C40-3	85	—	Chloride corrosion for 120 d
C60-3	125		
C0-1	0		
C40-1	85	CFRP reinforcement	—
C60-1	125		
C0-2	0		
C40-2	85	CFRP reinforcement	Chloride corrosion for 120 d
C60-2	125		

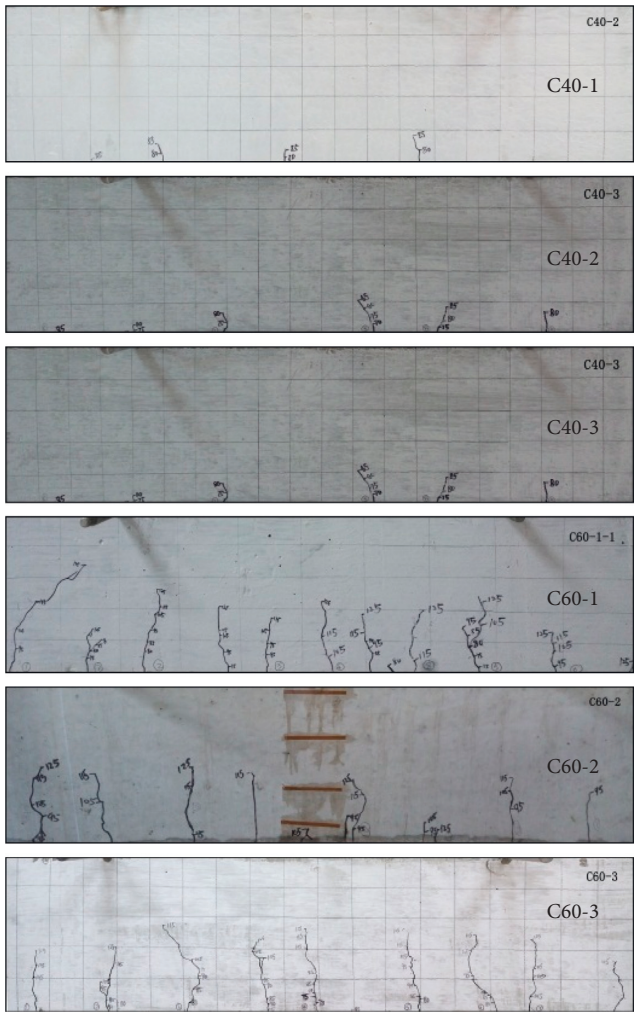

Figure 2: Initial cracks on the PC beams after preloading.

side of the beam was painted white and was marked with 5×5 cm grids to facilitate the detection of cracks.

3. Test Results and Discussion

3.1. Distribution of Cross-Sectional Strain. The strain distribution curves of PC beams are shown in Figure 6. In the approximately elastic stage, the strains of concrete at different heights are small and vary linearly. After cracking, the strains increase rapidly. And the section in the midspan, perpendicular to the beam longitudinal axis, is still plane after a pure bending deformation. It is found that the sectional strain at the midspan of the test beams still follows the plane section assumption after preloading, chloride corrosion, and CFRP reinforcement.

According to the strain distributions of beams C0-3, C40-3, C60-3, C0-2, C40-2, and C60-2, it can be seen that, after the immersion in chlorine salt for 120 d, the steel bars were corroded and expanded, resulting in microcracks in the surrounding concrete. During the loading process, the corrosion microcracks developed rapidly until the strain gauge failed. And the corrosion microcracks in the beam with the initial damage cracked earlier under the loading process. At the same time, CFRP pasted on the bottom has little effect on chloride corrosion.

It can be seen from Figure 6 that the ultimate compressive strain of control beam A1 and CFRP reinforced beams C0-1, C40-1, and C60-1, which are under natural conditions, is about 0.002. The ultimate compressive strain of CFRP reinforced beams C0-2, C40-2, and C60-2 in chloride condition is about 0.002. And the ultimate compressive strain of beams C0-3, C40-3, and C60-3 is about 0.001. It follows that the ultimate strain of concrete decreases with the corrosion of steel in the beam, and the

Table 2: Parameters of initial cracks on the midspan.

Beam	Crack number in midspan	Space (mm)	Sum of cracks (mm)	Crack width at bottom	Crack height (mm)
C40-1	4	150	6	0.04	40
C40-2	3	200	4	0.06	45
C40-3	3	170	6	0.06	50
C60-1	8	80	12	0.12	130
C60-2	7	100	11	0.12	125
C60-3	8	80	11	0.15	137

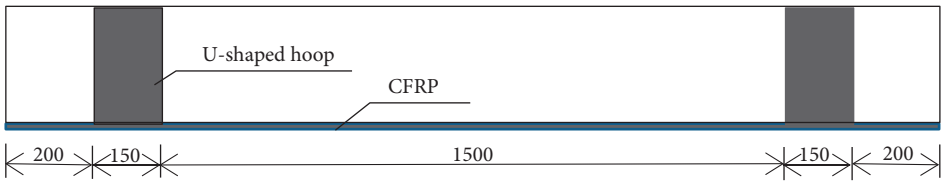

Figure 3: Reinforcing scheme of CFRP (unit: mm).

Table 3: Mechanical properties of CFRP.

Material	CFRP
Standard value of tensile strength	3493.5 MPa
Elasticity modulus	240 GPa
Elongation	1.7%
Bending strength	737.5 MPa
Shear strength	48.7 MPa
Positive tensile bond strength	3.6 MPa

Figure 4: Deicing salt corrosion.

reinforcement of CFRP decreases the effect of corrosion on the ultimate strain. Also, the relationship between the reduction of strain and corrosion and CFRP reinforcement remains to be studied.

With the increase of load grades, the neutral axis moved up from the middle of the beam. After cracking, the movement increases and the height of the compression zone decreases gradually. The compressive concrete depths of each PC beam under the ultimate load are shown in Figure 7. Under natural condition, the compressive concrete depth of the CFRP reinforced beam is higher than that of the control beam, and that of each beam decreased compared with that of the control beam under chloride corrosion for 120 d. Also, the compressive concrete depths of beams C0-1, C40-1, C60-1, C0-3, C40-3, and C60-3 decrease with the increase of the initial damage degree, while the law of C0-2, C40-2, and C60-2 is not obvious.

The chloride condition leads to the corrosion of the steel strand. As the corrosion degree increases, the sectional area of the steel strand decreases. The experiment in the literature [21] indicates that the corroded steel strand is more prone to slip during the bending test, and the slip rate and ultimate slip value increase with the corrosion degree. The bond slip between the steel strand and the concrete has occurred during the preloading process. Therefore, the bond performance between the steel strand and concrete has been weakened after preloaded to crack or corroded by chloride condition. And the tension stress of the steel strand decreased than that in the control beam under same load grade. For the CFRP reinforced beam, the section curvature and the arm of force between steel bars, steel strand, CFRP, and compressive concrete are smaller than those of the control beam under the action of equivalent load. It makes the neutral axis height lower than the control beam and the compressive concrete depth higher than the control beam. Also, the section curvature and the arm of force decrease with the increase of damage and corrosion degree. Due to the limited data and errors, the distribution of cross-sectional strains of PC beams and the variation in the compressive concrete depths under the action of multifactor are still to be studied.

3.2. Flexural Behavior

3.2.1. Load-Deflection Curves. According to the test results, the load-deflection curve of PC beams in the midspan is drawn, as shown in Figure 8. With the increase of load grade, the deflection in the midspan goes through three stages:

(1) In the approximate elastic stage, the deformation of the PC beam behaves linearly and slowly. However, the initial flexural stiffness of the beams decreases with initial damage, so the deformation rates of these beams in this stage are higher than that of the control beam. After chloride corrosion of 120 d, the stiffness of the beams decreases further and the deformation rates increase further than that of the control beam.

(2) In the cracking stage, the bottom concrete was loaded to crack and exited the work. CFRP gives play

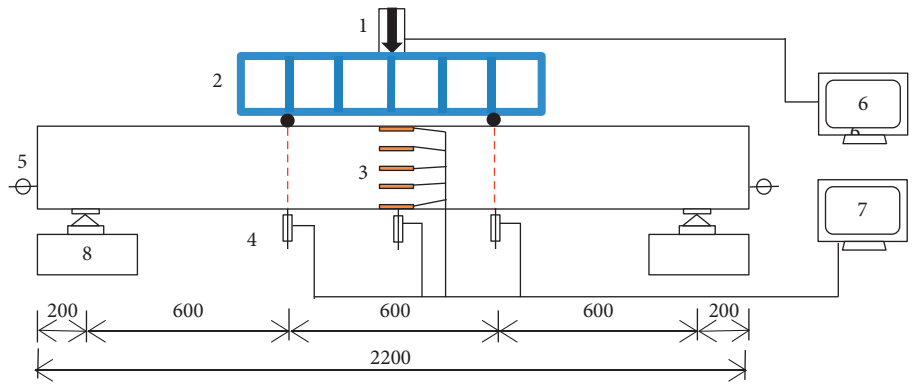

Figure 5: Loading test setup (unit: mm). Note: 1, load cell; 2, steel spreader beam; 3, strain gauge; 4, displacement sensor; 5, dial indicator; 6, computer; 7, data acquisition system.

to its high tensile strength, so that the stiffness degradation rate and the deformation rate of CFRP strengthened beam decrease. Under natural conditions, the initial damage has little effect on the flexural stiffness; however, the coupling of chloride corrosion and initial damage reduces the stiffness and accelerates the deformation of the structure in this stage.

(3) In the failure stage, the test beams yield and maintain a high bearing capacity, and the deflection in the midspan increases rapidly. Arriving at the ultimate bearing capacity, the structure is destroyed.

3.2.2. Flexural Stiffness. In order to analyze the degradation of the flexural stiffness of PC beams under different working conditions, all test beams are considered as homogeneous elastic material models. As the loading time is short and the deflections along the longitudinal sections are different, so the "minimum stiffness principle" is adopted. For the members under flexural load, the deflection is obtained by quadratic integration of curvature:

$$w = \iint \left(\frac{1}{\rho}\right)_x dx^2 = \iint \frac{M_x}{B_s} dx^2, \quad (1)$$

where w is the deflection, ρ is the radius of curvature, M_x is the bending moment of the beam plane, and B_s is the short-term stiffness. The midspan deflection of the test beam is obtained by solving the above integral. The test beam is simply supported by static loading at two points. The short-term stiffness of the test beam can be obtained by transforming the formula (1), as shown in the following formula:

$$B_s = S\frac{\left(M_x l_o^2\right)}{f} = S\frac{P l_o^3}{6f}, \quad (2)$$

where S is the deflection coefficient related to the supporting condition and load form, through calculation, the value of S is 23/216. P is the load value, f is the deflection in the midspan, and l_o is the calculated span.

According to formula (2), the short-term stiffness of the midspan section is calculated, as shown in Figure 9. Before cracking, the flexural stiffness of the test beams is basically unchanged, and the initial stiffness of the nondestructive beams C0-1, C0-2, and C0-3 is close to that of the control beam. Under the chloride condition, the initial flexural stiffness of beams C40-3 and C60-3 with initial cracks decreases by about 32.5% and 47.8% compared with the control beam and that of the CFRP reinforced beams C40-2 and C60-2 decreases by about 44.1% and 39.7%, respectively. Under the natural conditions, the initial stiffness of the CFRP reinforced beams C40-1 and C60-1 decreases by about 12.8% and 20.4%, respectively, compared with the control beam. After cracking, the stiffness of the test beams decreases with the increase of load grade. Moreover, the degradation rates of the stiffness of CFRP reinforced beam are lower than that of the control beam.

It can be seen that the change rule of the stiffness of the test beams is consistent with that of the deflection in the midspan. The initial flexural stiffness of the test beams is decreased due to the initial cracks. After the chloride corrosion, the cross-sectional areas of the internal steel bars and strands are decreased, the bond behaviors between the steel strand and concrete are weakened, and the effective prestress is decreased accordingly. Therefore, the flexural stiffness of the test beams decreases with the increase of damage degree under the same load grade. After strengthened by CFRP, CFRP exerts its high tensile performance in the cracking stage and inhibits the structural deformation, and the degradation rates of the flexural stiffness of the CFRP reinforced beams are reduced compared with the control beam. However, CFRP reinforcement has little effect on the initial flexural stiffness.

3.2.3. Cracking Load and Ultimate Load. The effective prestress of the PC beam is calculated according to the cracking load of midspan concrete, as shown in Table 4. It can be seen that the effective prestress and cracking load of control beam A1 are similar to the theoretical value. It can be considered that there is no sustained loss of effective prestress since the end of the curing period. However, after chloride corrosion of 120 d, the effective prestress of beam C0-3 decreased by 20% compared with the theoretical value,

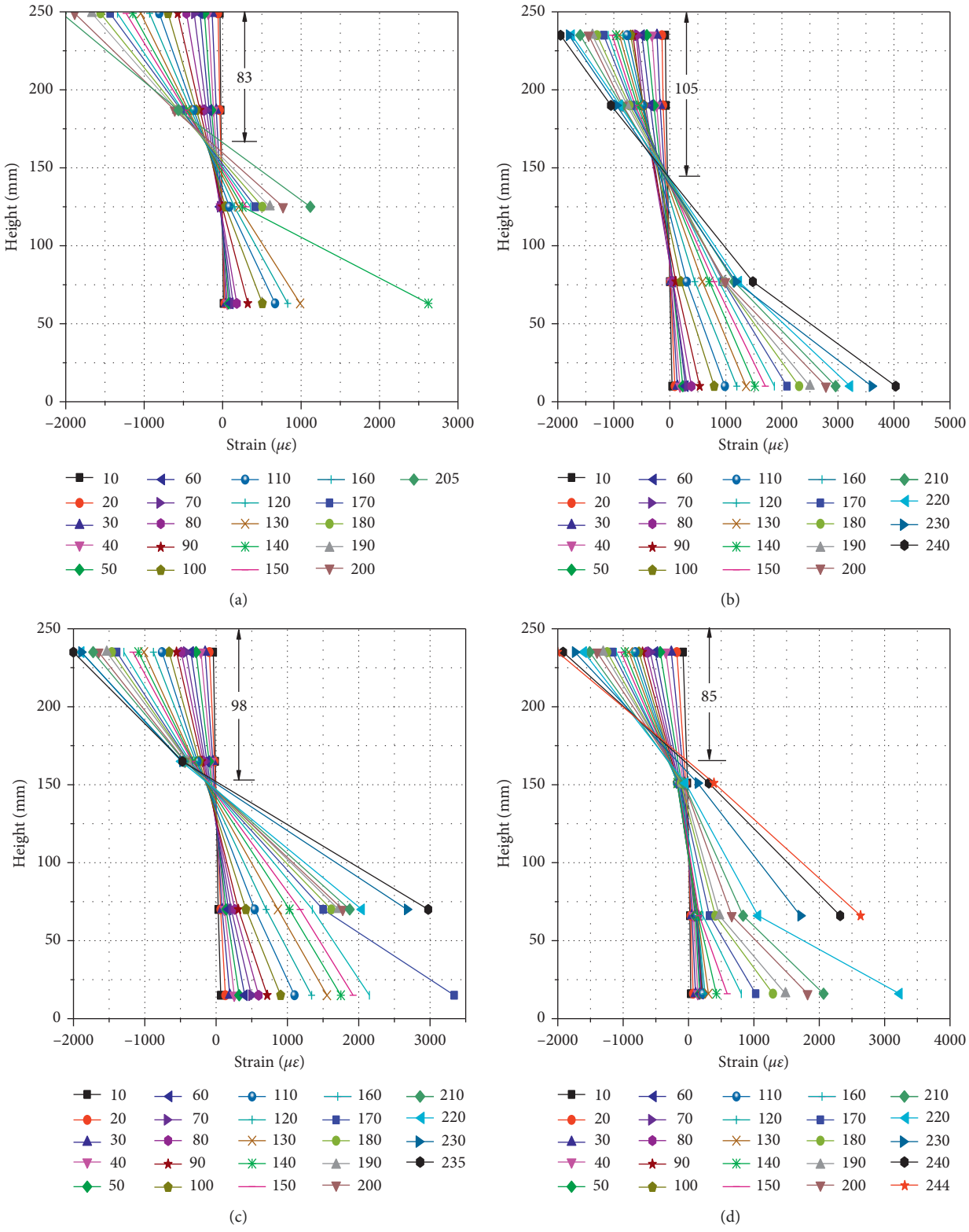

Figure 6: Continued.

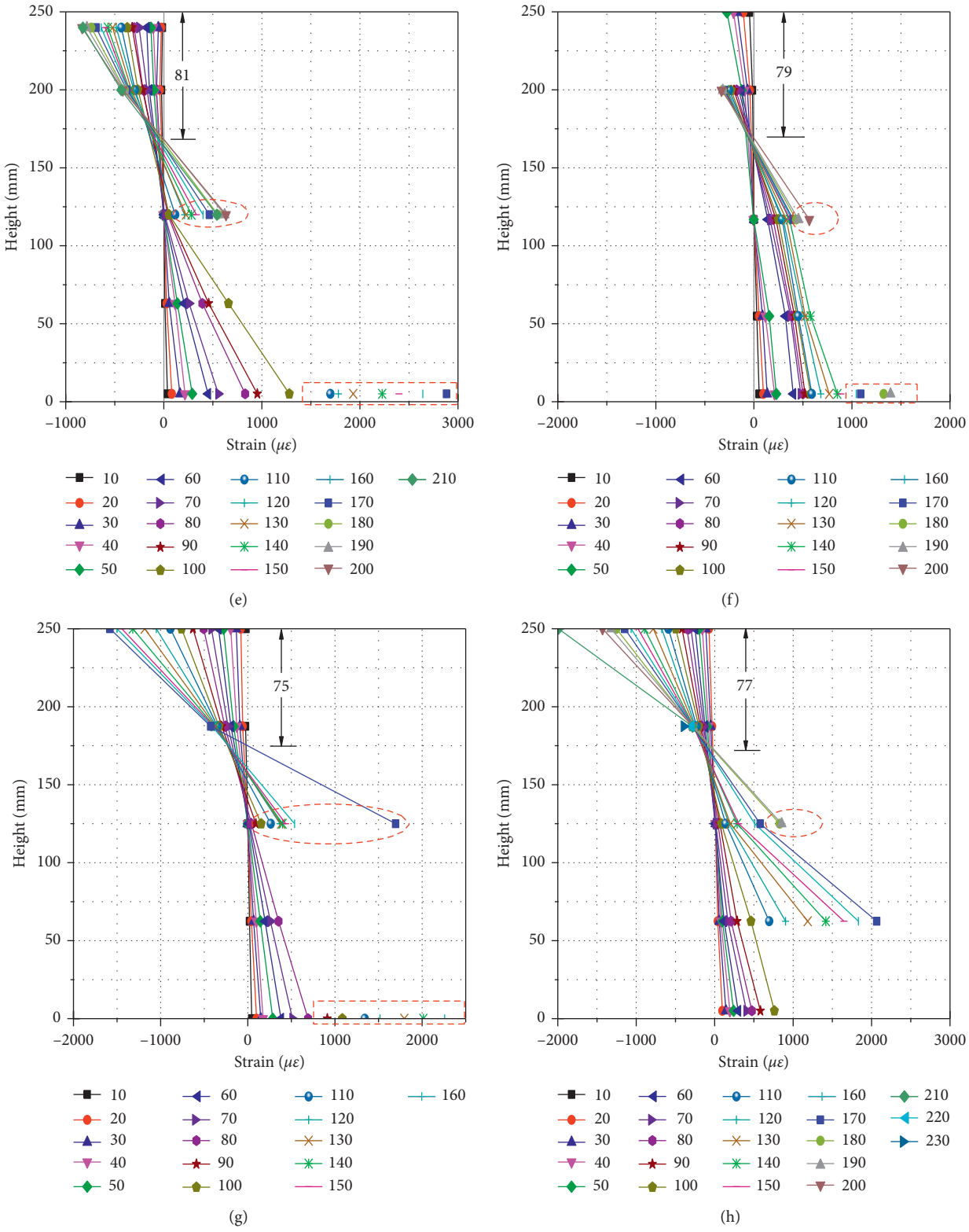

Figure 6: Continued.

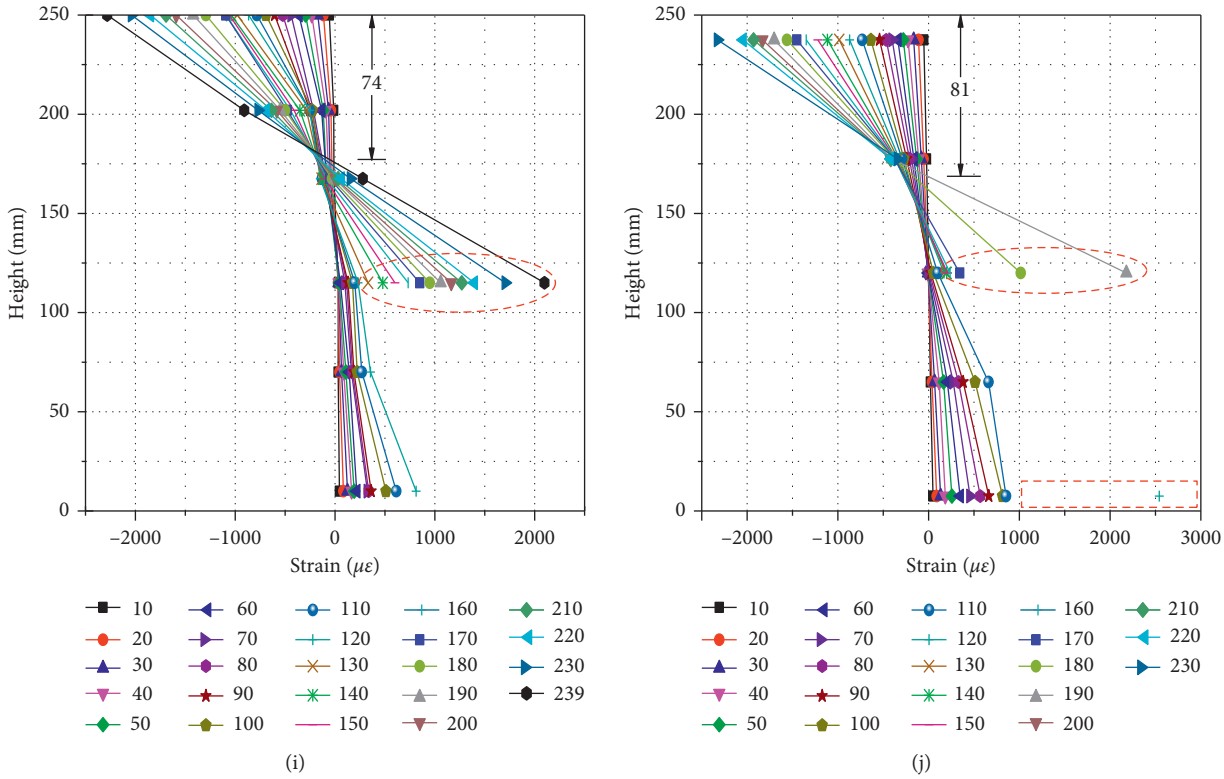

Figure 6: Distribution of strain at the midspan. (a) Beam A1, (b) beam C0-1, (c) beam C40-1, (d) beam C60-1, (e) beam C0-3, (f) beam C40-3, (g) beam C60-3, (h) beam B2, (i) beam C40-2, and (j) beam C60-2.

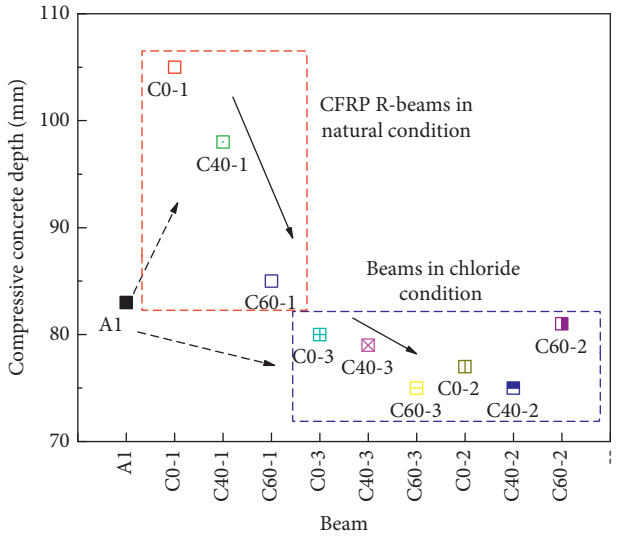

Figure 7: Compressive concrete depths at midspan.

and the cracking load decreased by 14%. It shows that the chloride corrosion on the steel strand leads to the degradation of its bond behavior with concrete.

The flexural behaviors of the test beams under the various working conditions are shown in Table 5. The cracking load of the test beams decreased after chloride corrosion and increased after the CFRP reinforcement compared with that of the control beams.

After chloride corrosion of 120 d, the ultimate loads of beams C0-3, C40-3, and C60-3 were reduced by 1.2%, 2.4%, and 9.0%, respectively, compared with the control beam A1. When the initial damage degree is low, the weakening effect of short-term chloride corrosion on the flexural behavior is not obvious, and the weakening effect increases with the initial damage degree. Under natural conditions, the ultimate loads of the CFRP reinforced beams were increased by 15.0%~18.7%. Under chloride condition, the ultimate loads of the CFRP reinforced beams were increased by 12.8%~16.2%. Chloride corrosion reduces the flexural capacity slightly. It is considered that the strengthening effect of CFRP significantly increases the flexural capacity, while the chloride corrosion and initial damage weaken the flexural behavior. When the three factors are coupled, the strengthening effect of CFRP is dominant compared with the weakening effect of chloride corrosion and initial damage.

3.2.4. Ductility. As can be seen from Table 5, CFRP pasted on the beam bottom exerts its high tensile strength to restrain the bending deformation, and ultimate deflection decreases. Therefore, the ductility of the CFRP reinforced beam decreases. Under the chloride condition, the structure with initial damage is more likely to be corroded by chloride, resulting in early failure of the structure. Therefore, the ultimate deflection and ductility are reduced significantly.

CFRP reinforcement can inhibit the structural deformation, but not reduce the chloride corrosion. Therefore,

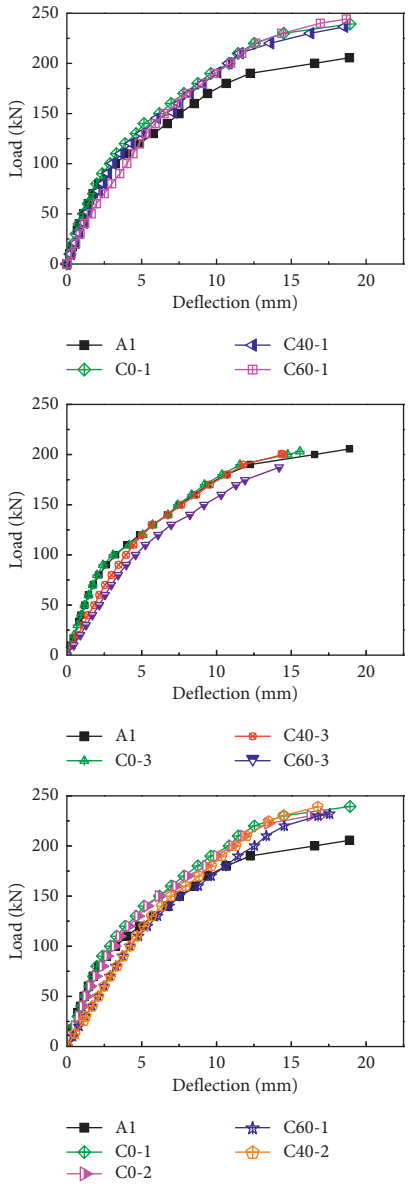

Figure 8: Load-deflection curves.

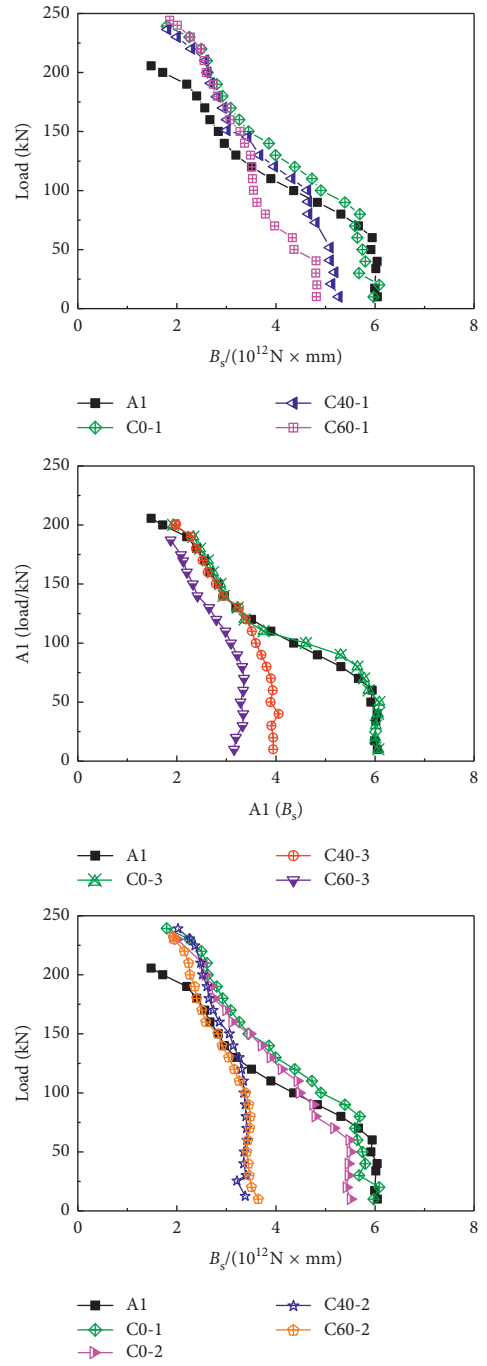

Figure 9: Flexural stiffness.

the ultimate deflection and ductility of the CFRP reinforced beams in chloride condition are further reduced than those of the control beams and slightly larger than those of unreinforced beams.

Due to the limited data, the changes in flexural capacity and ductility under the coupling of multiple factors still need to be further studied.

3.3. Cracking and Failure

3.3.1. Crack Patterns. During the loading process, new cracks appeared firstly in the middle span and below the loading points of the test beams. The cracks in the pure bending span developed vertically upward with the increase of load steps. When the neutral axis reached to the maximum height, the cracks are no longer continued. Then the oblique cracks in the shear spans extended rapidly. The distribution maps of cracks are shown in Figure 10. The parameters of cracks in the pure bending span are shown in Table 6.

During the cracking stage, initial cracks, CFRP reinforcement, and chloride corrosion all have impacts on the cracks of PC beams. According to their locations and causes, the cracks in Figure 10 can be divided into three categories, as is shown in Figure 11:

(1) Major cracks caused by bending stress appear in the midspan and below the loading points of the test beams. And the distribution of major cracks depends

Table 4: The effective prestress.

PC beam	Cracking load (kN)	Effective prestress (kN)
Theoretical value	70.3	1032.9
Control beam A1	70.0	1029.4
Beam C0-3	60.0	827.8

Table 5: Summary of the results.

No.	Rebound strength (MPa)	Cracking load (kN)	Ultimate load (kN)	Ultimate deflection (mm)	Yield load (kN)	Yield deflection (mm)	Ductility factor
A1	49.5	70	205.68	19.71	194.58	12.31	1.60
C0-1	49.6	80	239.28	18.92	220.02	12.53	1.51
C40-1	49.6	70/75	236.54	18.55	215.86	12.37	1.50
C60-1	50.5	75/95	244.23	18.69	224.26	13.29	1.41
C0-2	49.8	85	231.94	17.16	221.36	13.13	1.31
C40-2	48.4	70/75	239.02	16.77	228.05	13.27	1.26
C60-2	51.1	75/75	236.98	17.11	219.65	14.68	1.33
C0-3	51.2	60	203.20	15.57	187.29	11.03	1.41
C40-3	50.2	70/50	200.70	14.84	190.98	11.90	1.25
C60-3	51.2	70/60	187.25	14.18	174.70	11.74	1.21

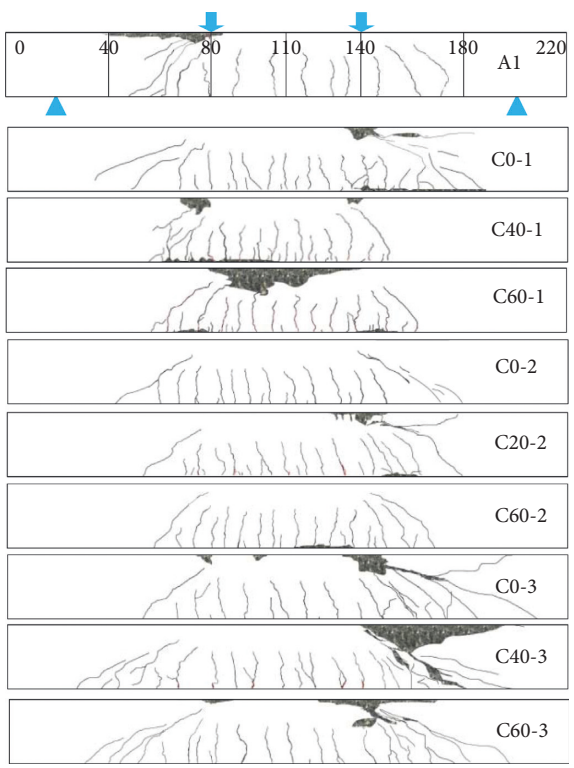

Figure 10: Distribution maps of cracks.

on the comprehensive bonding properties between the steel bar and concrete. Corrosion of steel bars caused by chloride leads to microcracks surrounded the steel bars. Bending stress makes the microcracks continue to develop and form the second type of major cracks. Therefore, such cracks occur above the corroded steel bars.

(2) Minor cracks occur near the major cracks. The local bond stress between concrete and CFRP increases with the increases of load. When the local tensile stress of concrete between major cracks reaches the ultimate tensile strength, the minor cracks appear between major cracks. Due to the low influence height of bond stress, such cracks are relatively short.

(3) CFRP peeling cracks are the third kind of cracks. Arriving at the ultimate load, there has a tendency of local peeling between the CFRP and concrete at the beam bottoms, and the peeling cracks are short and inclined or even parallel to the bottom surface and intersect with the major cracks and then cause the peeling off of the CFRP and concrete.

3.3.2. Failure Modes. The failure modes of the test beams are shown in Figure 12. In the bending test, the major cracks in the pure bending span of the control beam are vertically upward and evenly distributed with the increase of load grade. When the ultimate load is reached, the concrete beams A1, C0-1, C40-1, C60-1, and C40-2 are crushed.

Under the chloride condition, the crack patterns and the numbers of unreinforced beams C0-3, C40-3, and C60-3 are similar to that of the control beam, and part of the major cracks are developed from the position where the steel bars or strand was corroded. In addition, the reduction in the cross-sectional area of the steel bars and stirrups leads to the weakening of shear capacity. Arriving at the ultimate load, the oblique cracks are penetrated from the support to the loading point, leading to the concrete crushing at the loading point, and the compressive strength of the concrete on the midspan was not fully utilized. And the structure is subjected to shear failure.

Compared with the control beam, the surface cracks in the CFRP reinforced beams are denser, and there are more short minor cracks and peeling cracks. For example, under natural conditions, the crack numbers of the CFRP reinforced beams in the midspan are about 1.7~2.3 times that of

Table 6: Parameters of cracks in the pure bending span.

Beam	Number	Average spacing (mm)	Height (mm)	Maximum width (mm)	Crack patterns	Failure mode
A1	7	91	170	0.18	MAC	CCF
C0-1	15	45	150	0.12		
C40-1	16	39	165	0.28		CCF, CRF
C60-1	12	52	155	0.25	MAC, MIC, PEC	
C0-2	12	47	155	0.12		
C60-2	14	42	150	0.15		CCF, CRF
C40-2	12	52	162	0.11		
C0-3	8	80	165	0.24		
C60-3	8	77	160	0.22	MAC	CCF, CSF
C40-3	9	74	155	0.20		

Note. MAC, major crack; MIC, minor crack; PEC, CFRP peeling crack; CCF, concrete crush failure; CSF, concrete shear failure; CRF, CFRP rupture failure.

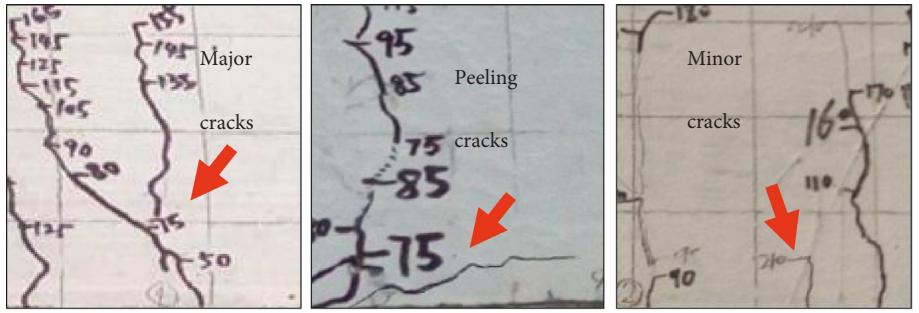

Figure 11: Classification of cracks.

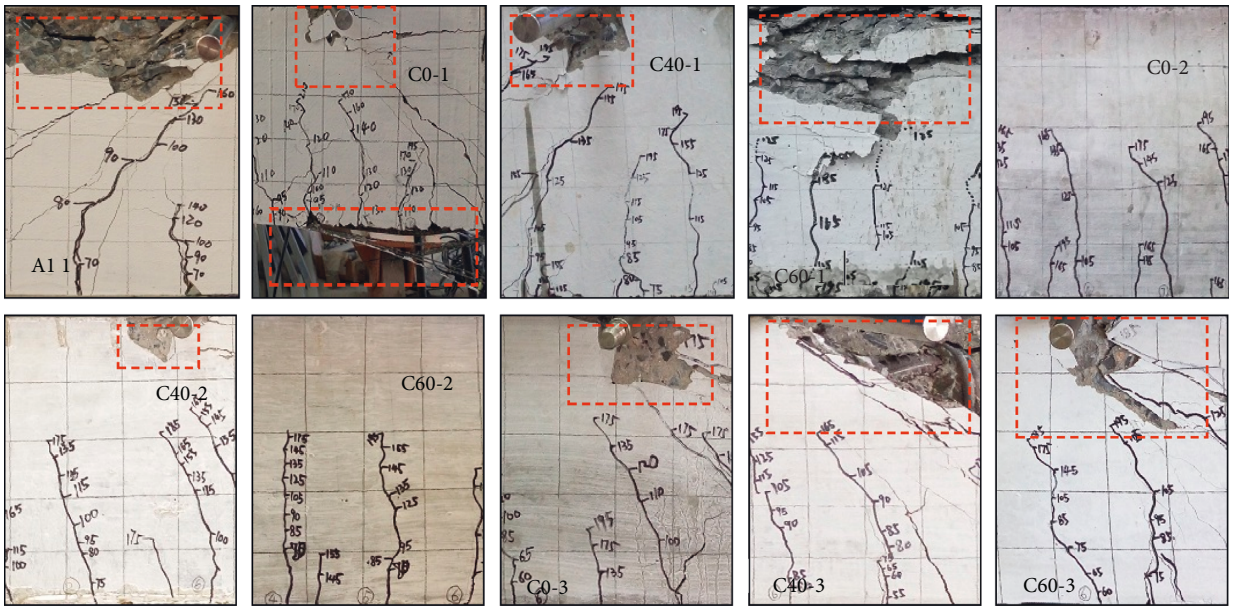

Figure 12: Failure modes of the test beams.

the control beam, and under chloride environment, the crack numbers of the CFRP reinforced beams in the midspan are about 1.5~2 times that of the control beam A1. Arriving at the ultimate load, the concrete of the CFRP reinforced beams in the midspan or under the loading point are crushed, and CFRP is fractured and peeled off. In this experiment, the damage on CFRP is not serious, which can prevent the concrete from disintegrated and falling off on a large scale.

3.3.3. Crack Widths. The average widths of the major cracks on different heights of PC beams are shown in Figure 8. It can be seen that the crack widths shift linearly with the

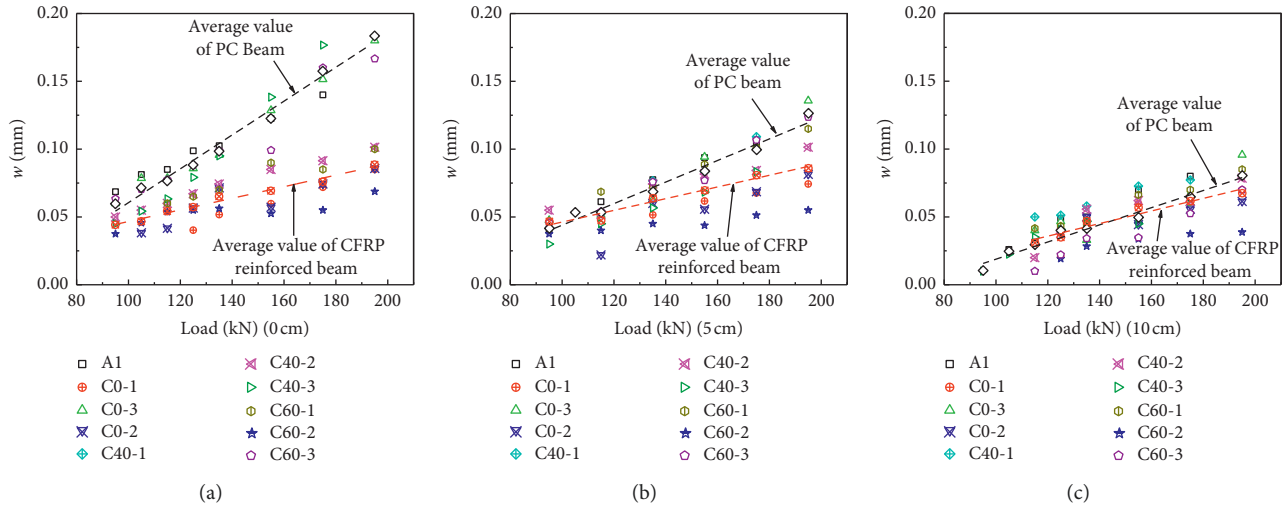

Figure 13: Crack widths and loads curves. (a) Average widths of cracks on the bottom, (b) at 5 cm, and (c) at 10 cm.

increase of load steps. The average widths of cracks on bottoms of CFRP strengthened beams C0-1, C0-2, C40-1, C40-2, C60-1, and C60-2 are all significantly smaller than that of the unreinforced beams A1, C0-3, C40-3, and C60-3. The cracking widths of the CFRP reinforced beams are slightly smaller than that of the unreinforced beams at a height of 5 cm from the beam bottom. At a height of 10 cm from the beam bottom, the gaps of the crack widths between the CFRP reinforced beams and the unreinforced beams are not obvious.

As can be seen from Figure 13, the reinforcement of CFRP has a greater impact on the development of cracks compared with initial damage and short-term chloride corrosion. Therefore, the average crack widths of CFRP reinforced and unreinforced beams were fitted with the linear method. When the load is 115 kN, the average crack widths of the CFRP reinforced beams at 0 cm, 5 cm, and 10 cm from the beam bottom decrease by 29%, 11%, and 5%, respectively, compared with that of the unreinforced beams. When the load is 195 kN, they decrease by 52.5%, 32.5%, and 17.5%, respectively. At the same time, the average crack widths of the unreinforced beams at 5 cm and 10 cm are 31.1% and 56.3% smaller than those at the bottom, while the average crack widths of the CFRP reinforced beams at 5 cm and 10 cm are only 3.1% and 24% smaller than those at the bottom.

The cracking rates of the test beams are shown in Figure 14. The cracking rates of unreinforced beam gradually decrease with the increase of cracking heights. For example, the cracking rate at the beam bottom is 1.25 μm/km, and the cracking rate at 5 cm and 10 cm decreased by 36.4% and 71.0%, respectively. The cracking rates of the CFRP reinforced beams at 0 cm, 5 cm, and 10 cm are almost same, and the cracking rates are 65.8%, 45.7%, and 26.7% lower than that of the unreinforced beams, respectively.

In conclusion, the average crack widths and cracking rates of the CFRP reinforced beams at the same heights are always smaller than those of the unreinforced beams, and the gaps between them increase with the load steps and decrease with the increase of crack heights. Initial damage and short-term

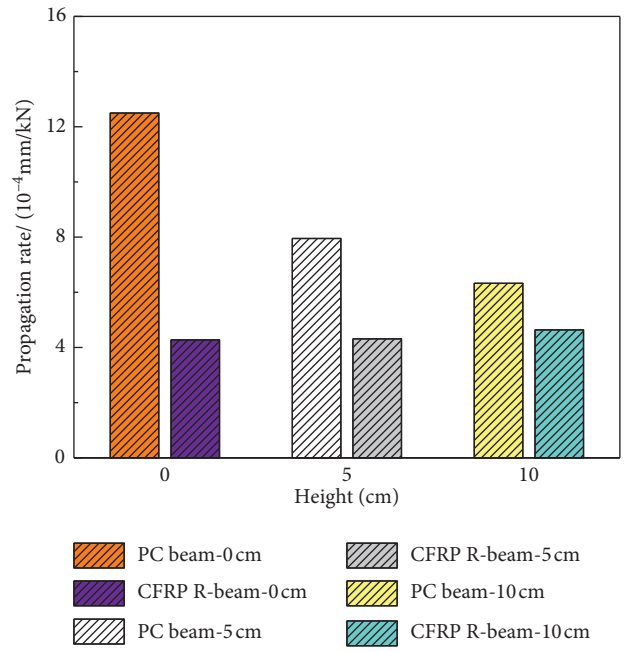

Figure 14: Cracking rates.

chloride corrosion have no obvious effects on the process of cracking. However, CFRP has a significant constraint on the development of cracks, and the effect decreases with the increase of crack heights. Also, the influence height of constraint is related to the thickness, layer numbers of CFRP, and other factors, which need to be further studied.

4. Conclusions

Ten pretensioned concrete beams designed with different test conditions were tested. And the effects of initial cracks, CFRP reinforcement, and chloride corrosion on the flexural behavior, cracking characteristics, and failure modes were discussed. The following conclusions can be drawn based on the test.

(1) Considering the initial cracks, chloride corrosion, and CFRP reinforcement, the sectional strain of the test beams still follows the plane section assumption after a pure bending deformation.

(2) The initial flexural stiffness is reduced by initial cracks and chloride corrosion, and CFRP reinforcement has little effect on the initial flexural stiffness. Before cracking, the flexural stiffness of the test beams is basically unchanged with the load steps. In the cracking stage, the stiffness decreases with the increase of load steps. And CFRP pasted on the beam bottom exerts its high tensile performance in this stage, inhibits the structural deformation, and reduces the degradation rate of flexural stiffness compared with the control beam.

(3) The effect of chloride corrosion increases with the degree of initial cracks. Under the chloride condition of 120 d, the effective prestress of the PC beams is weakened, cracking loads and ductility are reduced, and the ultimate loads are reduced by less than 10%. And the failure mode is prone to change from concrete crushing failure to shear failure. After the reinforcement of CFRP, the cracking loads of the test beams increase, the ductility of these beams is reduced compared to the control beam and increased compared to the chloride corrosion beams, and the ultimate loads increase than the control beam by 12.8%~18.7%. When the three factors are coupled, the enhancement effect of CFRP is more obvious than the weakening effects of short-term chloride corrosion and initial damage.

(4) CFRP reinforcement has a constraint effect on the development of cracks, and the effect decreases with the increases of crack height. Therefore, the average crack width and cracking rate of the CFRP reinforced beams at the same height are always smaller than those of the unreinforced beams. When the load grade is 195 kN, the average crack widths of the CFRP reinforced beams at 0 cm, 5 cm, and 10 cm from the beam bottom are 52.5%, 32.5%, and 17.5% smaller than that of the unreinforced beams, and the cracking rates are reduced by 65.8%, 45.7%, and 26.7%, respectively.

Data Availability

The data used to support the findings of this study are included within the article.

Conflicts of Interest

The authors declare that they have no conflicts of interest.

Acknowledgments

This work was conducted with the financial support from the National Natural Science Foundation of China (grant nos. 51578099 and 51178069). The support is gratefully acknowledged.

References

[1] M. P. Torill and R. E. Melchers, "Performance of 45-year-old corroded prestressed concrete beams," *Structures and Buildings*, vol. 166, pp. 547–559, 2013.

[2] P. Colajanni, A. Recupero, G. Ricciardi, and N. Spinella, "Failure by corrosion in PC bridges: a case history of a viaduct in Italy," *International Journal of Structural Integrity*, vol. 7, no. 2, pp. 181–193, 2016.

[3] F. Li, Y. Yuan, and C.-Q. Li, "Corrosion propagation of prestressing steel strands in concrete subject to chloride attack," *Construction and Building Materials*, vol. 25, no. 10, pp. 3878–3885, 2011.

[4] L. Wang, X. Zhang, J. Zhang, J. Yi, and Y. Liu, "Simplified model for corrosion-induced bond degradation between steel strand and concrete," *Journal of Materials in Civil Engineering*, vol. 29, no. 4, article 04016257, 2017.

[5] L. Wang, X. Zhang, J. Zhang, L. Dai, and Y. Liu, "Failure analysis of corroded PC beams under flexural load considering bond degradation," *Engineering Failure Analysis*, vol. 73, pp. 11–24, 2017.

[6] F. Li and Y. Yuan, "Effects of corrosion on bond behavior between steel strand and concrete," *Construction and Building Materials*, vol. 38, pp. 413–422, 2013.

[7] F.-M. Li and Y.-S. Yuan, "Experimental study on bending property of prestressed concrete beams with corroded steel strands," *Journal of Building Structures*, vol. 31, no. 2, pp. 78–84, 2010.

[8] Z. Rinaldi, S. Imperatore, and C. Valente, "Experimental evaluation of the flexural behavior of corroded P/C beams," *Construction and Building Materials*, vol. 24, no. 11, pp. 2267–2278, 2010.

[9] X. Zhang, L. Wang, J. Zhang, Y. Ma, and Y. Liu, "Flexural behavior of bonded post-tensioned concrete beams under strand corrosion," *Nuclear Engineering and Design*, vol. 313, pp. 414–424, 2017.

[10] R. Yang, J. Zhang, L. Wang et al., "Experimental research for flexural behavior on concrete beams with local corrosion fracture of strands," *Journal of Central South University (Science and Technology)*, vol. 49, no. 10, pp. 2593–2601, 2018.

[11] M. A. Vicente, D. C. González, and J. A. Martínez, "Mechanical response of partially prestressed precast concrete I-beams after high-range cyclic loading," *Practice Periodical on Structural Design and Construction*, vol. 20, no. 1, pp. 1–22, 2015.

[12] A. Recupero and N. Spinella, "Preliminary results of flexural tests on corroded prestressed concrete beams," in *Proceedings of the Fib Symposium 2019: CONCRETE-Innovations in Materials, Design and Structures*, pp. 1323–1330, Kraków, Poland, May 2019.

[13] A. Dasar, R. Irmawaty, H. Hamada, Y. Sagawa, and D. Yamamoto, "Prestress loss and bending capacity of precracked 40 year-old PC beams exposed to marine environment," *Matec WEB of Conferences*, vol. 47, article 02008, 2016.

[14] N. Spinella, P. Colajanni, A. Recupero, and F. Tondolo, "Ultimate shear of RC beams with corroded stirrups and strengthened with FRP," *Buildings*, vol. 9, no. 2, p. 34, 2019.

[15] E. M. Adham and S. Khaled, "Flexural behavior of corroded pretensioned girders repaired with CFRP sheets," *PCI Journal*, vol. 59, no. 2, pp. 129–143, 2014.

[16] I. Shaw and B. Andrawes, "Repair of damaged end regions of PC beams using externally bonded FRP shear reinforcement," *Construction and Building Materials*, vol. 148, pp. 184–194, 2017.

[17] L. K. Jarret, K. A. Harries, R. Miller, and R. J. Brinkman, "Repair of prestressed-concrete girders combining internal strand splicing and externally bonded CFRP techniques," *Journal of Bridge Engineering*, vol. 19, no. 2, pp. 200–209, 2014.

[18] E. R. Calvin and R. J. Peterman, "Evaluation of prestressed concrete girders strengthened with carbon fiber reinforced polymer sheets," *Journal of Bridge Engineering*, vol. 9, no. 2, pp. 185–192, 2004.

[19] D. Cerullo, K. Sennah, H. Azimi, C. Lam, A. Fam, and B. Tharmabala, "Experimental study on full-scale pretensioned bridge girder damaged by vehicle impact and repaired with fiber-reinforced polymer technology," *Journal of Composites for Construction*, vol. 17, no. 5, pp. 662–672, 2013.

[20] A. Elsafty, M. K. Graeff, and S. Fallaha, "Behavior of laterally damaged prestressed concrete bridge girders repaired with CFRP laminates under static and fatigue loading," *International Journal of Concrete Structures and Materials*, vol. 8, no. 1, pp. 43–59, 2014.

[21] Y. Liu, Y. Fan, J. Yu et al., "Flexural behavior test of corroded prestressed concrete beams under chloride environment," *Acta Materiae Compositae Sinica* no. 37, In press, in Chinese.